RESEARCH ARTICLE

Hydrodynamic Assessment of Alternative Channel Geometry and Flood Mitigation Designs Using HEC-RAS 2D: Implications for Sustainable Urban Drainage Systems.

Dhanush Raghupathy
Cascade Civil Services LLC
Email: dhanushunionly@gmail.com

Received	Revised	Accepted	Published
22 May 2025	29 June 2025	18 August 2025	15 September 2025

Abstract

Background: Channel rehabilitation is frequently judged by nominal conveyance gains, although the same geometry may yield different overbank behaviour and urban exposure under escalating design floods.

Objective: This study compares an existing trapezoidal channel with 20% widening, a depth increase represented by a 1.17 bankfull-depth multiplier, compound benches, and hybrid rehabilitation in a structured HEC-RAS 2D-oriented hydraulic scenario assessment.

Methods: The record comprises 18 cross-sections, 108 floodplain cells of 1 ha each and 25 geometry–event combinations with 10-, 25-, 50-, 100- and 500-year peak flows of 39–116 m³/s.

Results: Mean bankfull capacity increases from 63.46 m³/s in the existing channel to 75.35, 83.42, 86.89 and 113.88 m³/s, respectively. At 100 years, mapped inundation declines from 60 ha in the existing case to 36 ha with widening and 0 ha with the other three alternatives at the recorded 0.05-m depth-screening threshold. At 500 years, existing, widened, deepened and compound-channel scenarios inundate 96, 84, 72 and 72 ha; the hybrid scenario has no cell exceeding the screening threshold. However, 10 of 18 hybrid cross-sections still exhibit overbank flow, while mean channel velocity rises from 2.267 to 2.317 m/s.

Conclusion: The results distinguish areal inundation, local capacity exceedance and velocity response, demonstrating that a dry screened raster is not equivalent to elimination of hydraulic risk. Geometry-only intervention screening should therefore precede, rather than substitute for, calibrated design verification and integrated urban drainage assessment.

Keywords: Channel rehabilitation; HEC-RAS 2D; floodplain modelling; channel conveyance; urban drainage; overbank flow; hydrodynamic assessment.

How to cite: Raghupathy D. Hydrodynamic Assessment of Alternative Channel Geometry and Flood Mitigation Designs Using HEC-RAS 2D: Implications for Sustainable Urban Drainage Systems. Int J Bus Comput Sci. 2025.

1. Introduction

Urban drainage performance is governed not only by peak discharge but also by channel cross-sectional geometry, roughness, floodplain connectivity and the location of exposed land uses. Numerical floodplain models can quantify the interaction of these controls, while differences in spatial discretisation and urban obstruction representation can materially affect predicted inundation [1]–[5]. Laboratory-supported HEC-RAS 2D applications and recent investigations of depth-averaged equations further show why water depth and flow pathways should be evaluated together rather than using a single conveyance indicator [6], [7].

Widening, deepening and compound sections modify hydraulic radius, velocity, wetted perimeter and local discharge thresholds differently. Their performance can therefore change with event magnitude: an alternative controlling a moderate flood may still overtop during a rarer event. Spatial resolution and longitudinal channel representation also affect the interpretation of mapped inundation [8], [9].

Sustainable urban drainage extends beyond conveyance to runoff attenuation, water quality and system resilience [10]–[12]. Reviews and grey–green studies support combining structural improvements with distributed storage and source controls [13]–[17]. Capacity gains alone therefore do not establish that channel rehabilitation is sustainable or that it reduces every relevant hazard.

We compare five channel configurations under 10-, 25-, 50-, 100- and 500-year design discharges, quantifying bankfull capacity, overbank sections, mapped inundation, urban exposure and velocity. The objectives are to identify event-dependent differences among interventions and distinguish screened flood reductions from verified hydraulic safety.

2. Materials and Methods

2.1 Hydraulic Reach and Analytical Inputs

The domain contains 18 cross-sections along 4.25 km at 250-m intervals. Existing bottom width is 11.40–12.80 m, bankfull depth 2.15–2.37 m, Manning n 0.0340–0.0415 and local energy slope 0.00220–0.00256; side slopes are 1.25 H:1 V. Mean bankfull capacity is 63.46 m³/s. The 1.2 km × 0.9 km floodplain comprises 108 one-hectare cells with elevations 108.686–110.188 m, of which 72 are classified as urban.

The 120-month hydroclimatic record includes rainfall, wet-day counts, extreme 24-h rainfall, potential evapotranspiration and soil moisture. The five specified events have 24-h rainfall of 78, 102, 128, 154 and 224 mm; corresponding peak inputs are 39, 54, 68, 83 and 116 m³/s. Each has a 12-h peak-duration parameter. These are design inputs, not outcomes of a documented fitted rainfall–runoff model.

2.2 Channel Rehabilitation Alternatives

The alternatives are existing geometry (E); 20% bottom widening (W); bankfull depth ×1.17 (D), equivalent to approximately 0.37–0.40 m additional depth; compound benches (C), with width ×1.12, depth ×1.08, side slope ×1.30 and n ×0.97; and hybrid rehabilitation (H), with width ×1.24, depth ×1.15, side slope ×1.25 and n ×0.90. Unspecified factors remain at 1.00. These parameterised alternatives have not been cost-optimised.

The section-level bankfull capacities average 75.35, 83.42, 86.89 and 113.88 m³/s for W, D, C and H, respectively: 18.7%, 31.5%, 36.9% and 79.4% above E. These capacities follow the specified geometry and roughness changes; Table 1 records the design assumptions.

2.3 Hydraulic Response and Raster Screening

The HEC-RAS 2D-oriented archive records 25 design cases, each with 18 section responses and 108 raster-cell responses. Section data include discharge, water depth and level, mean velocity, bankfull capacity, surcharge and overbank flags. Cells contain depth, velocity, hazard index, urban status and wet flags. The shallow-water conservation framework underlying two-dimensional hydraulic models is described in [3], [4]. Native model files, mesh settings and solver diagnostics are absent, so numerical convergence is not independently established.

Mapped inundation is $A_s = 1\ \text{ha} \times \Sigma_i\, I(d_i,s > 0.05\ \text{m})$, consistent with the stored wet-cell flags. Urban exposure is $\Sigma_i\, I(d_i,s > 0.05\ \text{m})U_i$, where U_i is the urban indicator. Overbank count is $N_s = \Sigma_j\, O_j,s$ for 18 sections. Flood-area reduction is $100(A_E - A_s)/A_E$ when baseline $A_E > 0$. It is undefined for the 10- and 25-year cases, which have zero mapped area.

Maximum grid depth includes subthreshold traces; mean channel velocity averages 18 section values. All 450 section and 2,700 cell records were independently reconciled with the 25-case summary for flooded areas, urban exposure and overtopping counts. No sampling-based tests are appropriate for these deterministic design cases.

2.4 Comparative and Design Interpretation

Comparison focuses on mean conveyance, overbank section counts, mapped inundation, urban wet cells, depth and mean channel velocity. Particular attention is given to the 100- and 500-year cases. A dry classified cell does not prove zero water depth, and no flood damage, erosion loss or monetary benefit is inferred without supporting records [18]–[23].

3. Results

3.1 Conveyance Capacity and Onset of Overtopping

No section exceeds bankfull at 10 years (39 m³/s). At 25 years (54 m³/s), only E overtops, at one section. The 50-year event (68 m³/s) produces overbank flow at 14 of 18 E sections, three W sections, one D section and none under C or H. Thus W still has local exceedances despite its mean 75.35-m³/s capacity exceeding the imposed 68-m³/s discharge (Table 2; Figure 2).

At 100 years (83 m³/s), all E sections are overbank, compared with 14 W, 10 D, six C and zero H sections. At 500 years (116 m³/s), all 18 sections exceed bankfull under E, W, D and C; only H reduces the total, to 10. The H design therefore shows the clearest improvement in local capacity exceedance while still retaining a non-negligible exceedance count during the rarest event. Figure 4 displays the associated mean capacity increases.

3.2 Floodplain Inundation and Urban Exposure

All configurations have zero wet cells at 10 and 25 years. At 50 years, E inundates 36 ha, all designated urban; no alternative exceeds the 0.05-m wet threshold. At 100 years, E inundates 60 ha and W 36 ha (40% less); D, C and H have no threshold-exceeding cells (Table 2; Figure 1). Yet D and C still have ten and six overtopped sections, respectively: section exceedance does not always produce wet cells in the stored grid.

At the 500-year input, the existing geometry inundates 96 ha, including all 72 urban-flagged cells. W reduces inundation to 84 ha (12.5%) but leaves 72 urban wet cells. D and C both inundate 72 ha (25.0% less than E), again with all 72 urban cells exposed. H has no grid cells flagged as wet, equivalent to a 100% reduction in *screened* area compared with E, despite 10 overbank sections. Twelve H cells contain numerical depths of 0.001 m, below the screening threshold. The analysis therefore distinguishes screened surface exposure from local overbank exceedance and trace-depth fields (Figure 3).

3.3 Depth Attenuation and Residual Hydraulics

The maximum gridded depth at 100 years is 0.428 m for E and 0.212 m for W; D, C and H have no recorded depth exceedance above the 0.05-m threshold. At 500 years, the maximum depth decreases from 0.928 m in E to 0.668 m in W, 0.580 m in D and 0.475 m in C, before reaching a 0.001-m numerical trace in H. Among the wet grid cells, mean depths decline from 0.497 m (E) to 0.368 m (W), 0.350 m (D) and 0.269 m (C) at 500 years. Thus C and D have identical flood extents but different hydraulic depths, a distinction lost in an area-only comparison.

The velocity response is not uniformly decreasing. At 500 years, mean section velocity is 2.267 m/s for E, 2.209 m/s for W, 2.267 m/s for D, 2.224 m/s for C and 2.317 m/s for H. Hybrid rehabilitation raises the mean by 0.050 m/s (2.2%) compared with E even while reducing the mapped flood footprint. At 100 years, the corresponding values are 2.050, 1.988, 2.050, 2.008 and 2.085 m/s. These results indicate a hydraulic trade-off between improved conveyance and retained in-channel flow intensity (Table 3; Figure 4).

4. Discussion

Channel capacity improvements delay overbank initiation but depend on bottleneck sections, not reach-mean capacity alone. W raises mean conveyance by 18.7% yet retains three overbank sections at 50 years. This supports evaluating longitudinal geometry rather than treating a single average capacity as a design guarantee [3], [8], [9].

Deepening and compound benches produce the same 72-ha extent at 500 years but not the same hydraulic intensity. C reduces maximum depth to 0.475 m versus 0.580 m under D and mean channel velocity to 2.224 versus 2.267 m/s. Area-only appraisals therefore miss relevant depth and velocity differences [5]–[7], [19], [20]. Sediment and shear-stress records would be needed to assess scour.

The H alternative raises mean bankfull capacity by 79.4% and delivers the smallest mapped area, yet still exceeds bankfull at 10 sections during the 500-year event. Twelve cells retain depths of 0.001 m, below the 0.05-m wet threshold. Thus 100% reduction in *screened* area does not establish absence of overflow. Mean section velocity is also 2.2% higher than E, warranting reach-specific checks of hydraulic transitions and bed protection before implementation.

Sustainability also requires runoff quality, amenity, ecological performance and long-term operation. Conventional widening or deepening need not improve these functions. Distributed retention and integrated grey–green solutions may complement conveyance improvements [10]–[17]. These alternatives should be appraised within the wider urban drainage system, not judged solely as channel earthworks.

The 100-year D and C scenarios have no threshold-exceeding cells despite local overbank flow. At 500 years, all 72 urban-flagged cells remain wet in E, W, D and C despite variations in total area. Thus affected hectares cannot substitute for asset-level depth, duration, vulnerability or damage estimates [21], [24]–[29]. Multiple hydraulic and exposure metrics are needed for credible design comparisons.

H provides the strongest hydraulic screening outcome, while C may be attractive where reduced peak depth and velocity matter. The ranking is conditional because construction cost, footprint, maintenance, ecological effects and downstream backwater were not analysed. Broader sustainability objectives could alter the preferred design [12]–[17], [30].

5. Conclusion

Across 25 geometry–event cases, mean bankfull capacity increases from 63.46 m³/s under existing conditions to 113.88 m³/s under hybrid rehabilitation. At 100 years, mapped inundation declines from 60 ha to 36 ha with widening and to zero wet cells under deepening, compound benches and hybrid modification. At 500 years, E, W, D, C and H inundate 96, 84, 72, 72 and 0 ha, respectively, at the 0.05-m screening threshold. Crucially, H retains 10 overbank sections and a 2.2% greater mean channel velocity than E. Channel geometry should therefore be evaluated through capacity, overtopping, depth and exposure jointly, followed by calibrated hydraulic and sustainability appraisal.

References

1. E. Mignot and B. Dewals, "Hydraulic modelling of inland urban flooding: Recent advances," Journal of Hydrology, vol. 609, art. 127763, 2022, doi: 10.1016/j.jhydrol.2022.127763.
2. J. Teng, A. J. Jakeman, J. Vaze, B. F. W. Croke, D. Dutta, and S. Kim, "Flood inundation modelling: A review of methods, recent advances and uncertainty analysis," Environmental Modelling & Software, vol. 90, pp. 201–216, 2017, doi: 10.1016/j.envsoft.2017.01.006.
3. M. S. Horritt and P. D. Bates, "Evaluation of 1D and 2D numerical models for predicting river flood inundation," Journal of Hydrology, vol. 268, pp. 87–99, 2002, doi: 10.1016/S0022-1694(02)00121-X.
4. P. D. Bates, M. S. Horritt, and T. J. Fewtrell, "A simple inertial formulation of the shallow water equations for efficient two-dimensional flood inundation modelling," Journal of Hydrology, vol. 387, pp. 33–45, 2010, doi: 10.1016/j.jhydrol.2010.03.027.
5. J. E. Schubert and B. F. Sanders, "Building treatments for urban flood inundation models and implications for predictive skill and modeling efficiency," Advances in Water Resources, vol. 41, pp. 49–64, 2012, doi: 10.1016/j.advwatres.2012.02.012.
6. A. Mustafa and M. Szydłowski, "Application of different building representation techniques in HEC-RAS 2-D for urban flood modeling using the Toce River experimental case," PeerJ, vol. 9, art. e11667, 2021, doi: 10.7717/peerj.11667.
7. B. Dewals et al., "Can the 2D shallow water equations model flow intrusion into buildings during urban floods?," Journal of Hydrology, vol. 619, art. 129231, 2023, doi: 10.1016/j.jhydrol.2023.129231.
8. T. J. Fewtrell, P. D. Bates, M. S. Horritt, and N. M. Hunter, "Evaluating the effect of scale in flood inundation modelling in urban environments," Hydrological Processes, vol. 22, pp. 5107–5118, 2008, doi: 10.1002/hyp.7148.
9. J. Neal, G. Schumann, and P. Bates, "A subgrid channel model for simulating river hydraulics and floodplain inundation over large and data sparse areas," Water Resources Research, vol. 48, art. W11506, 2012, doi: 10.1029/2012WR012514.
10. T. D. Fletcher et al., "SUDS, LID, BMPs, WSUD and more—The evolution and application of terminology surrounding urban drainage," Urban Water Journal, vol. 12, no. 7, pp. 525–542, 2015, doi: 10.1080/1573062X.2014.916314.
11. Q. Zhou, "A review of sustainable urban drainage systems considering the climate change and urbanization impacts," Water, vol. 6, no. 4, pp. 976–992, 2014, doi: 10.3390/w6040976.
12. K. Eckart, Z. McPhee, and T. Bolisetti, "Performance and implementation of low impact development—A review," Science of the Total Environment, vols. 607–608, pp. 413–432, 2017, doi: 10.1016/j.scitotenv.2017.06.254.
13. J. L. Webber et al., "Is green infrastructure a viable strategy for managing urban surface water flooding?," Urban Water Journal, vol. 17, pp. 598–608, 2020, doi: 10.1080/1573062X.2019.1700286.
14. J. Li, J. Zeng, G. Huang, and W. Chen, "Urban flood mitigation strategies with coupled gray–green measures: A case study in Guangzhou City, China," International Journal of Disaster Risk Science, vol. 15, no. 3, pp. 467–479, 2024, doi: 10.1007/s13753-024-00566-6.
15. M. Esraz-Ul-Zannat, A. Dedekorkut-Howes, and E. A. Morgan, "A review of nature-based infrastructures and their effectiveness for urban flood risk mitigation," WIREs Climate Change, vol. 15, no. 5, art. e889, 2024, doi: 10.1002/wcc.889.
16. D. Green, E. O'Donnell, and M. Johnson, "Green infrastructure: The future of urban flood risk management?," WIREs Water, vol. 8, art. e1560, 2021, doi: 10.1002/wat2.1560.
17. L. Li, P. Uyttenhove, and V. Van Eetvelde, "Planning green infrastructure to mitigate urban surface water flooding risk—A methodology to identify priority areas applied in the city of Ghent," Landscape and Urban Planning, vol. 194, art. 103703, 2020, doi: 10.1016/j.landurbplan.2019.103703.
18. A. Alipour, K. Jafarzadegan, and H. Moradkhani, "Global sensitivity analysis in hydrodynamic modeling and flood inundation mapping," Environmental Modelling & Software, vol. 152, art. 105398, 2022, doi: 10.1016/j.envsoft.2022.105398.
19. F. Dottori, P. Salamon, A. Bianchi, L. Alfieri, F. A. Hirpa, and L. Feyen, "Development and evaluation of a framework for global flood hazard mapping," Advances in Water Resources, vol. 94, pp. 87–102, 2016, doi: 10.1016/j.advwatres.2016.05.002.
20. C. C. Sampson, A. M. Smith, P. D. Bates, J. C. Neal, L. Alfieri, and J. E. Freer, "A high-resolution global flood hazard model," Water Resources Research, vol. 51, pp. 7358–7381, 2015, doi: 10.1002/2015WR016954.
21. J. C. Neal et al., "Distributed whole city water level measurements from the Carlisle 2005 urban flood event and comparison with hydraulic model simulations," Journal of Hydrology, vol. 368, pp. 42–55, 2009, doi: 10.1016/j.jhydrol.2009.01.026.
22. G. Aronica, P. D. Bates, and M. S. Horritt, "Assessing the uncertainty in distributed model predictions using observed binary pattern information within GLUE," Hydrological Processes, vol. 16, pp. 2001–2016, 2002, doi: 10.1002/hyp.398.
23. F. Pappenberger, K. Frodsham, K. Beven, R. Romanowicz, and P. Matgen, "Fuzzy set approach to calibrating distributed flood inundation models using remote sensing observations," Hydrology and Earth System Sciences, vol. 11, pp. 739–752, 2007, doi: 10.5194/hess-11-739-2007.
24. B. Merz, J. Hall, M. Disse, and A. Schumann, "Fluvial flood risk management in a changing world," Natural Hazards and Earth System Sciences, vol. 10, pp. 509–527, 2010, doi: 10.5194/nhess-10-509-2010.
25. P. Scussolini et al., "FLOPROS: An evolving global database of flood protection standards," Natural Hazards and Earth System Sciences, vol. 16, pp. 1049–1061, 2016, doi: 10.5194/nhess-16-1049-2016.
26. E. E. Koks, B. Jongman, T. G. Husby, and W. J. W. Botzen, "Combining hazard, exposure and social vulnerability to provide lessons for flood risk management," Environmental Science & Policy, vol. 47, pp. 42–52, 2015, doi: 10.1016/j.envsci.2014.10.013.
27. H. C. Winsemius et al., "Global drivers of future river flood risk," Nature Climate Change, vol. 6, pp. 381–385, 2016, doi: 10.1038/nclimate2893.
28. O. E. J. Wing et al., "Estimates of present and future flood risk in the conterminous United States," Environmental Research Letters, vol. 13, art. 034023, 2018, doi: 10.1088/1748-9326/aaac65.
29. P. D. Bates and A. P. J. De Roo, "A simple raster-based model for flood inundation simulation," Journal of Hydrology, vol. 236, pp. 54–77, 2000, doi: 10.1016/S0022-1694(00)00278-X.
30. C. Agonafir et al., "A review of recent advances in urban flood research," Water Security, vol. 19, art. 100141, 2023, doi: 10.1016/j.wasec.2023.100141.

Figures

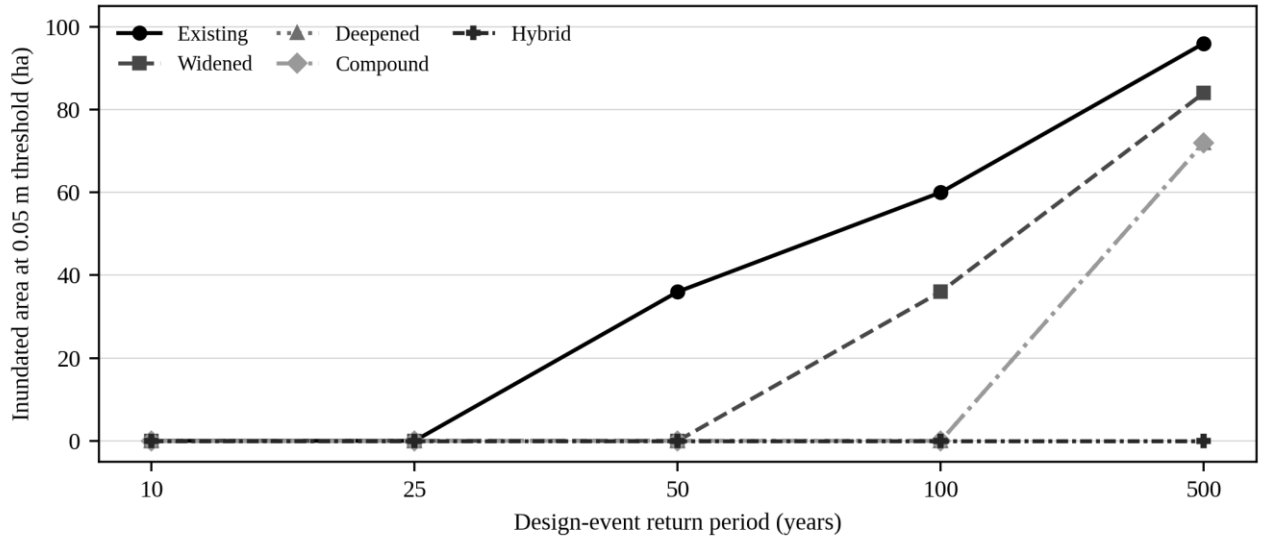

Figure 1. Floodplain inundation by event return period and channel configuration using the recorded 0.05-m wet-cell threshold. Zero indicates no threshold-exceeding cells, not necessarily zero numerical depth.

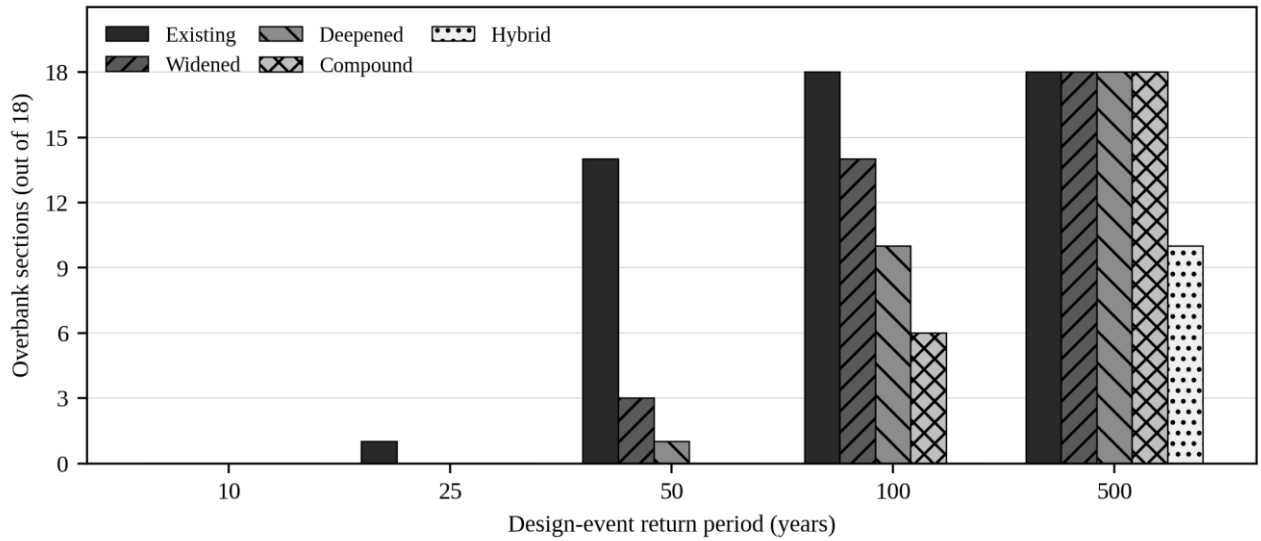

Figure 2. Number of cross-sections exceeding local bankfull depth for each alternative. Each scenario contains 18 section records; the hybrid configuration retains 10 overbank sections in the 500-year event.

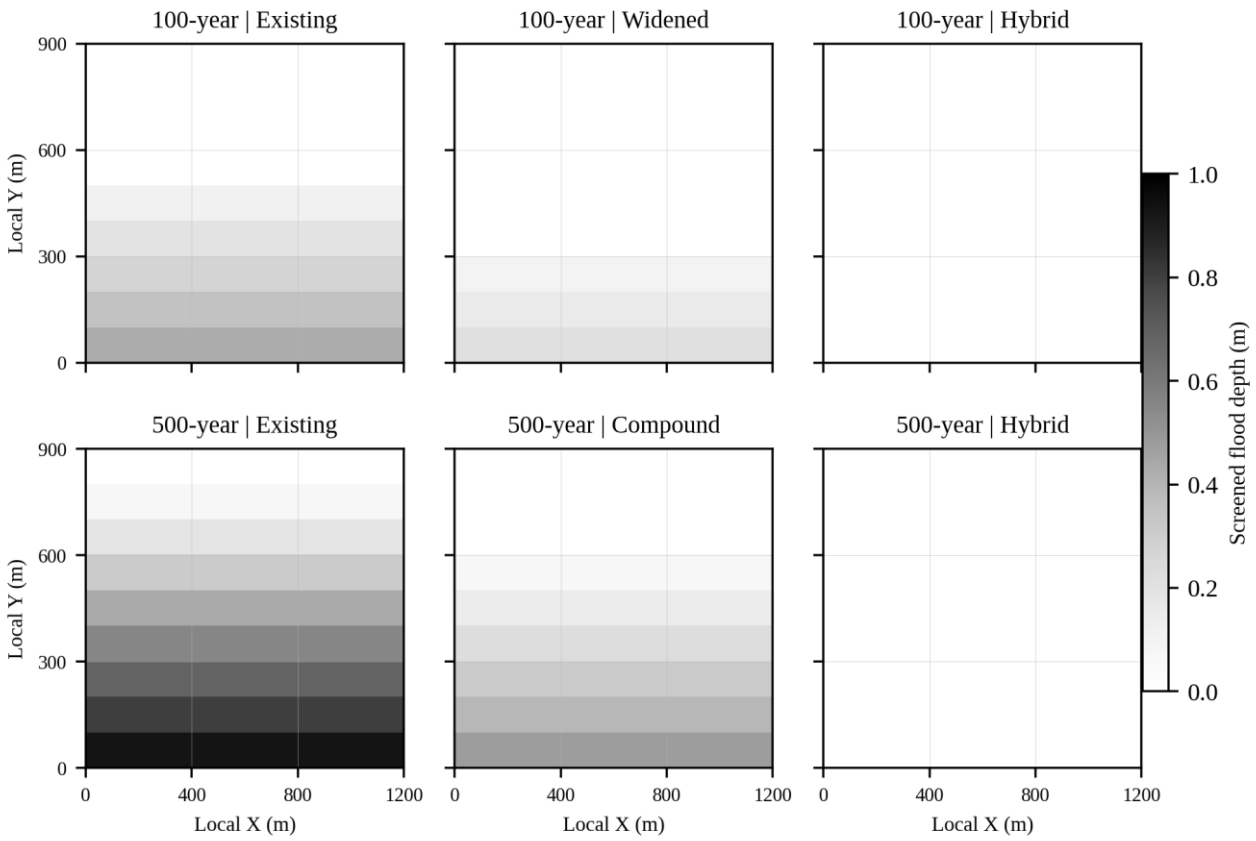

Figure 3. Screened maximum flood-depth grids for 100- and 500-year events. The 100-m raster uses a common grayscale depth scale. White cells are at or below the 0.05-m inundation threshold.

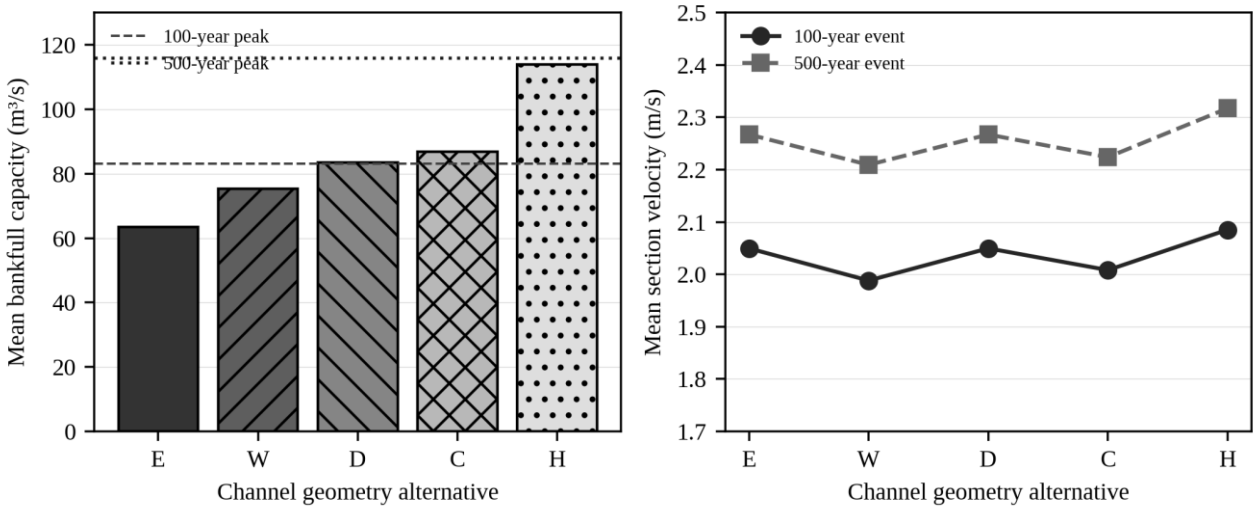

Figure 4. Comparison of mean bankfull capacity with 100- and 500-year design discharges (left) and mean channel velocities at those events (right). E = existing, W = widened, D = deepened, C = compound, H = hybrid.

Tables

Table 1. Hydraulic domain, design forcing and channel alternatives

Parameter	Definition
Channel and floodplain	18 sections over 4.25 km; 108 cells of 100 m × 100 m (108 ha)
Existing cross-section	Bottom width 11.40–12.80 m; bankfull depth 2.15–2.37 m; side slope H:V = 1.25:1
Hydraulic coefficients	Manning n 0.0340–0.0415; energy slope 0.00220–0.00256
Design peak Q (m³/s)	39, 54, 68, 83 and 116 at 10, 25, 50, 100 and 500 years
Existing (E)	Width, bankfull depth, side slope, roughness multipliers 1.00 each
Widened (W)	Width ×1.20; depth ×1.00; side slope ×1.00; n ×1.00
Deepened (D)	Width ×1.00; depth ×1.17; side slope ×1.00; n ×1.00
Compound benches (C)	Width ×1.12; depth ×1.08; side slope ×1.30; n ×0.97
Hybrid rehabilitation (H)	Width ×1.24; depth ×1.15; side slope ×1.25; n ×0.90
Mapped flood-cell criterion	Stored wet flag; depth greater than 0.05 m per 1-ha raster cell

Table 2. Matched-event channel capacity, inundation and urban exposure

RP (yr)	Alt.	Mean Qcap (m³/s)	Flooded (ha)	Max grid d (m)	Overbank (n)	Urban wet (n)	Mean V (m/s)
10	E	63.46	0	0.000	0	0	1.614
10	W	75.35	0	0.000	0	0	1.550
10	D	83.42	0	0.000	0	0	1.614
10	C	86.89	0	0.000	0	0	1.578
10	H	113.88	0	0.000	0	0	1.626
25	E	63.46	0	0.000	1	0	1.792
25	W	75.35	0	0.000	0	0	1.729
25	D	83.42	0	0.000	0	0	1.792
25	C	86.89	0	0.000	0	0	1.754
25	H	113.88	0	0.000	0	0	1.813
50	E	63.46	36	0.184	14	36	1.927
50	W	75.35	0	0.000	3	0	1.865
50	D	83.42	0	0.000	1	0	1.927
50	C	86.89	0	0.000	0	0	1.887
50	H	113.88	0	0.000	0	0	1.956
100	E	63.46	60	0.428	18	60	2.050
100	W	75.35	36	0.212	14	36	1.988
100	D	83.42	0	0.000	10	0	2.050
100	C	86.89	0	0.000	6	0	2.008
100	H	113.88	0	0.000	0	0	2.085
500	E	63.46	96	0.928	18	72	2.267
500	W	75.35	84	0.668	18	72	2.209
500	D	83.42	72	0.580	18	72	2.267
500	C	86.89	72	0.475	18	72	2.224
500	H	113.88	0	0.001	10	0	2.317

Table 3. Alternative performance relative to existing channel

RP (yr)	Alt.	Area reduction (%)	Overbank sections	Change in urban wet cells	Peak grid depth reduction (%)	Mean V change (%)
50	W	100.0	3/18	-36	100.0	-3.3
50	D	100.0	1/18	-36	100.0	+0.0
50	C	100.0	0/18	-36	100.0	-2.1
50	H	100.0	0/18	-36	100.0	+1.5
100	W	40.0	14/18	-24	50.5	-3.0
100	D	100.0	10/18	-60	100.0	+0.0
100	C	100.0	6/18	-60	100.0	-2.0
100	H	100.0	0/18	-60	100.0	+1.7
500	W	12.5	18/18	+0	28.0	-2.6
500	D	25.0	18/18	+0	37.5	+0.0
500	C	25.0	18/18	+0	48.8	-1.9
500	H	100.0	10/18	-72	99.9	+2.2